Separation Science and Technology
Publication details, including instructions for authors and subscription information:
http://www.informaworld.com/smpp/title~content=t713708471

Groundwater Cleanup by *in-situ* Sparging. I. Mathematical Modeling

David J. Wilson[a]; Satoshi Kayano[a]; Robert D. Mutch Jr[b]; Ann N. Clarke[b]
[a] DEPARTMENTS OF CHEMISTRY AND OF CIVIL ENVIRONMENTAL ENGINEERING, VANDERBILT UNIVERSITY, NASHVILLE, TENNESSEE [b] ECKENFELDER, INC. 227 FRENCH LANDING DRIVE, NASHVILLE, TENNESSEE

To cite this Article Wilson, David J. , Kayano, Satoshi , Mutch Jr, Robert D. and Clarke, Ann N.(1992) 'Groundwater Cleanup by *in-situ* Sparging. I. Mathematical Modeling', Separation Science and Technology, 27: 8, 1023 — 1041
To link to this Article: DOI: 10.1080/01496399208019022
URL: http://dx.doi.org/10.1080/01496399208019022

SEPARATION SCIENCE AND TECHNOLOGY, 27(8 & 9), pp. 1023–1041, 1992

Groundwater Cleanup by *in-situ* Sparging. I. Mathematical Modeling

DAVID J. WILSON* and SATOSHI KAYANO

DEPARTMENTS OF CHEMISTRY AND OF CIVIL AND ENVIRONMENTAL ENGINEERING
VANDERBILT UNIVERSITY
NASHVILLE, TENNESSEE 37235

ROBERT D. MUTCH, JR. and ANN N. CLARKE

ECKENFELDER, INC.
227 FRENCH LANDING DRIVE
NASHVILLE, TENNESSEE 37228

Abstract

The technique of *in-situ* sparging may provide a cheaper and more rapid method for removal of volatile organic compounds (VOCs) from groundwater than conventional pump and treat operations. A local equilibrium model is developed to describe *in-situ* sparging by means of a horizontal lateral slotted pipe at the bottom of a trench filled with crushed rock and normal to the direction of flow of the groundwater. The effects of air flow rate, groundwater flow rate, aquifer thickness, number of theoretical transfer units (related to axial dispersion), Henry's constant of the VOC, and initial VOC concentration are explored. Also, a method is developed for using vadose zone soil gas pressure measurements in the vicinity of a single sparging well to estimate the radius of influence of the well.

INTRODUCTION

The pump and treat method is the oldest and probably most widely used of the techniques for remediating sites contaminated with toxic chemicals in which groundwater is involved. This method is satisfactory if the contaminant is relatively soluble in water and if the aquifer medium has a permeability that is relatively constant. The method is less satisfactory if the contaminant is of low solubility in water, so that nonaqueous phase liquid (NAPL) may be present, and/or if the permeability of the medium

*To whom correspondence should be addressed.

is highly variable (i.e., fractured porous rock, clay lenses in sand or gravel, etc.). In the first case the rate of equilibration between the droplets/ganglia of NAPL and the mobile aqueous phase may be rather slow, and in the second, diffusion of contaminant from stagnant pore water in the porous domains of low permeability into the mobile water may be severely rate-limiting. In either case, cleanup will be slow, with prolonged tailing; rebound of contaminant concentration in the groundwater may also be observed after pump and treat operations are stopped. Naymik (*1*) included a discussion on fractured porous media in a review on the dynamics of groundwater. A common approach has been to use a dual porosity model, with high porosity and generally low permeability for the porous blocks and low porosity and high permeability for the fracture system (*2–5*).

Weber and his associates (*6*) recently published a study of nonequilibrium dissolution of NAPLs in subsurface systems. They noted the importance of nonequilibrium effects in the solution of "blobs" of NAPL in advecting groundwater, and ascribed these to 1) rate-limited mass transport between the nonaqueous and aqueous phases, 2) by-passing of the advecting aqueous phase around contaminated regions having a low aqueous phase permeability, and 3) nonuniform flow due to aquifer heterogeneities.

We have examined the implications of matrix diffusion effects for the clean up of fractured porous rock and other heterogeneous aquifers (*7–9*). Under quite reasonable circumstances the remediation of such aquifers by conventional pump and treat methods was estimated by means of a mathematical model to take decades to centuries.

Many of the sites of interest are contaminated with VOCs of low water solubility from leaking underground storage tanks (*10*), spills, improper waste disposal, etc. In the vadose zone one can take advantage of the volatility of these compounds to remove them by soil vapor extraction, but this technique cannot be used below the water table (*11*). In pump and treat operations the extracted groundwater is usually treated biologically or by means of air stripping for the removal of these VOCs.

Recently Herrling and Stamm (*12*) described the use of vacuum-vaporizer wells for *in-situ* removal of strippable VOCs in the vadose and saturated zones. This technology is now established in Germany, and these workers presented both a mathematical model for design purposes and experimental results. At the same meeting Brown (*13*) described the use of a simpler configuration (simple air injection or sparging wells) which Ground Water Technology, Inc., has used successfully in the United States for the *in-situ* removal of VOCs from contaminated groundwater.

In these techniques, both of which are sparging methods, one uses air injection to generate convective currents in the aquifer in the vicinity of

the well to increase local turbulence (thereby enhancing mass transport from NAPL droplets and ganglia) and to provide a vapor-phase route for the efficient removal of VOC from the aquifer. This contaminated soil gas can then be captured for treatment by any of the methods used in soil vapor extraction, or, if the VOCs are biodegradable, they might be destroyed by soil microorganisms as the injected gas moves up through the vadose zone.

In the next section we develop a simple mathematical model for the operation of an aeration curtain sparging system for the removal of VOCs from an aquifer. This system is envisioned as a trench excavated to the bottom of the aquifer at right angles to the natural direction of flow of the groundwater, at the bottom of which lies a horizontal slotted pipe, which is overlain with coarse gravel or crushed rock. Compressed air is blown through the horizontal slotted pipe, sparging the groundwater as it slowly moves across the aeration curtain. The curtain is designed to intercept the plume of contaminated groundwater leaving the site.

This is followed by an analysis of the dependence of the soil gas pressure distribution in the vadose zone above a sparging well. A point of interest which arises with such systems is the effective radius of the aeration cone (the radius at the top of the aquifer of the zone of aeration surrounding the well). It was hoped that measurement of the soil gas pressures near the bottom of the vadose zone would provide a method by which one could estimate the radius of the aeration cone for various well designs and air flow rates. This, in fact, appears to be the case.

In-situ SPARGING WITH AN AERATION CURTAIN

The geometry of the proposed system is indicated in Fig. 1. The symbols are defined as follows.

L = thickness of aquifer (m)
a = width of aeration curtain (m)
c = length of aeration curtain (m)
n = number of equivalent theoretical transfer units into which the aeration curtain is partitioned for analysis
b = thickness of an equivalent theoretical transfer unit (m)
Q_w = total water flow rate through the curtain (m^3/s)
Q_a = total air flow rate through the curtain (m^3/s)
c_0 = incoming aqueous contaminant concentration (kg/m^3)
K_H = Henry's constant of the contaminant, dimensionless
ν = voids fraction in the crushed rock/gravel curtain, dimensionless

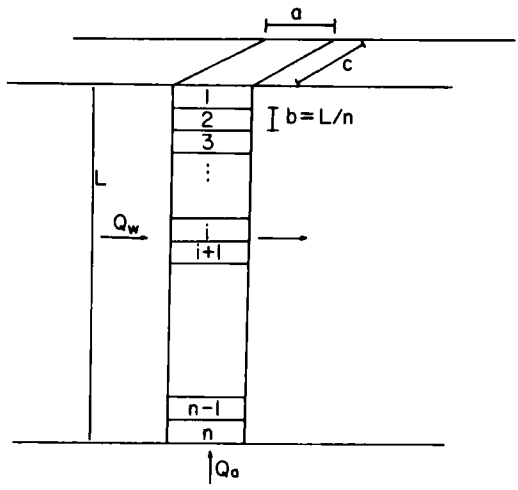

FIG. 1. The aeration curtain. Geometry and notation.

The hydrostatic pressure at the bottom of the ith cell (transfer unit) is given by

$$P_i = (1 + ib/10.336) \text{ atm} \tag{1}$$

so the volumetric airflow rate at the bottom of the jth cell is given by

$$Q_j^a = \frac{Q_a}{1 + jb/10.336} \tag{2}$$

We shall neglect the volume of air compared to the volume of water in a cell. Let m_i = mass of contaminant in the ith cell (kg). Then

$$\frac{dm_i}{dt} = \frac{Q_w}{n}(c_0 - c_i^w) + Q_i^a c_{i+1}^a - Q_{i-1}^a c_i^a \tag{3}$$

Making the steady-state assumption for the system then permits us to set Eq. (3) equal to zero.

Henry's law is assumed to apply to the VOC in the aquifer, which yields

$$c_j^a = K_H c_j^w, \qquad j = 1, 2, \ldots, n \tag{4}$$

Substitution of Eqs. (2) and (4) into Eq. (3) then gives

$$0 = \frac{Q_w}{n}(c_0 - c_i^w) + \frac{Q_a K_H c_{i+1}^w}{1 + ib/10.336} - \frac{Q_a K_H c_i^w}{1 + (i-1)b/10.336} \quad (5)$$

Solving Eq. (5) for c_i^w then yields

$$c_i^w = \left[\frac{Q_w c_0}{n} + \frac{Q_a K_H c_{i+1}^w}{1 + ib/10.336}\right] \Big/ \left[\frac{Q_w}{n} + \frac{Q_a K_H}{1 + (i-1)b/10.336}\right],$$

$$i = 1, 2, \ldots, n-1 \quad (6)$$

and

$$c_n^w = \frac{Q_w c_0}{n} \Big/ \left[\frac{Q_w}{n} + \frac{Q_a K_H}{1 + (n-1)b/10.336}\right] \quad (7)$$

The mean contaminant concentration in the water which has passed through the curtain is given by

$$\bar{c}_{out} = \sum_{i=1}^{n} c_i^w/n \quad (8)$$

and the percent removal of VOC from the passing groundwater by the curtain is

$$R = 100(1 - \bar{c}_{out}/c_0) \quad (9)$$

We next explore the dependence of R, the percent removal of VOC by the aeration curtain, on the parameters of the model. The default parameters used in the calculations are given in Table 1.

The effect of air flow rate is shown in Table 2. The expected increase in percent VOC removal with increasing air flow rate is observed, but, unlike the situation with countercurrent aerators, there is no abrupt transition. If the percent VOC removal is not adequate at a flow rate which is near the maximum feasible, a marginal increase in flow rate is not going to solve the problem.

The impact of the flow rate of the groundwater in the aquifer is given in Table 3. The expected decrease of percent VOC removal with increasing groundwater flow rate is seen, and again we find that there is no fairly

TABLE 1
Default Parameters Used in the Aeration Curtain Model

Depth of aquifer	5 m
Thickness of aeration curtain	0.5 m
Length of aeration curtain	100 m
Number of theoretical transfer units	10
Voids fraction of the crushed rock curtain	0.4
Contaminant	Trichloroethylene
Henry's constant of contaminant (15°C)	0.2821
Contaminant concentration in groundwater incident on the aeration curtain	100 mg/L
Total water flow across the aeration curtain	0.1 m^3/s
Total air flow rate generating the curtain	2 m^3/s

abrupt transition to an overloaded condition such as is found with countercurrent separations. The geometry of the aeration curtain is such that this is a crosscurrent separation method.

The number of theoretical transfer units used to represent the column was found to have only a minor effect on the percent VOC removal, as seen in Table 4. Since this is a crosscurrent separation, this was to be expected. The result also indicates that there is little to be gained from efforts to reduce longitudinal dispersion in the air in the curtain. The model assumes complete mixing across the thickness of the curtain for both vapor and aqueous phases. Unless the curtain is uneconomically thick, this is likely to be a reasonable assumption.

One expects the percent VOC removal to be independent of the VOC concentration of the groundwater entering the curtain since the modeling equations are all linear in the concentrations. Runs made with values of c_0 of 10, 100, and 1000 mg/L showed that this was precisely the case. Failure of the model to yield this result would have been proof of the existence of a bug in the program.

TABLE 2
Effect of Air Flow Rate on Percent VOC Removal

Air flow rate (m^3/s)	Percent VOC removal
0.5	67.02
1.0	80.96
1.5	86.64
2.0	89.71
3.0	92.96
5.0	95.68

TABLE 3
Effect of Groundwater Flow Rate on Percent VOC Removal

Groundwater flow rate (m^3/s)	Percent VOC removal
0.02	97.80
0.025	97.27
0.05	94.65
0.10	89.71
0.15	85.16
0.20	80.96
0.50	61.43

One might expect that there would be no dependence of percent VOC removal on aquifer thickness so long as the air and groundwater flow rates and the height of a theoretical transfer unit are held constant. As seen in Table 5, this is approximately, but not exactly, true. The air flow rate, Q_a, is at a pressure of 1 atm while the gas in any particular cell in the curtain is subject to additional pressure from the hydrostatic head of the curtain. Therefore the flow rate of the gas passing through the lower portions of the curtain is correspondingly reduced; the greater the depth, the greater the reduction. This in turn results in a slight decrease in the amount of VOC which can be removed from the thicker aquifers, as seen in Table 5.

The effect of the Henry's constant value on the percent VOC removal is of particular interest, since VOCs of interest show a rather wide range of Henry's constant values. This point is explored in Table 6. The Henry's constant for TCE (trichloroethylene) at 15°C was adapted from Howe, Mullins, and Rogers (*14*).

An inspection of the Henry's constants compiled by these authors shows that, while some VOCs have K_H values which are larger than 1.0 and many have K_Hs which are larger than 0.1, there are a number which have Henry's

TABLE 4
Effect of the Number of Theoretical Transfer Units n on Percent VOC Removal

n	Percent VOC removal
20	90.05
10	89.71
5	89.06
3	88.25

TABLE 5
Effect of Aquifer Thickness on Percent VOC Removal

Aquifer thickness (m)	Percent VOC removal
3	89.73
5	89.71
10	88.87

constants at 15°C which are substantially less than 0.1. A few of these are 1,2-dichlorobenzene (0.060), 1,2-dichloroethane (0.055), 1,1,2-trichloroethane (0.027), tetralin (0.044), ethylene dibromide (0.020), 1,2-dichloropropane (0.053), dibromochloromethane (0.019), 1,2,4-trichlorobenzene (0.044), methyl ethyl ketone (0.016), and methyl isobutyl ketone (0.016). The results of Table 6 raise some doubt as to the suitability of the aeration curtain technique for such compounds.

It was mentioned above that this is a crosscurrent technique. This means that the aeration curtain is, in essence, a single-stage technique. One might expect to improve its performance rather substantially by using a system having several aeration curtains in series and, indeed, this turns out to be the case. A simple analysis yields Eq. (10) for R_n, the percent VOC removal resulting from n aeration curtains in series.

$$R_n = 100[1 - (1 - R/100)^n] \tag{10}$$

Table 7 shows the effect of using multiple aeration curtain systems. It is apparent that the useful range of the aeration curtain technique can be extended substantially by employing multiple curtains. These need to be separated only enough to ensure that there is no movement of sparging air from one curtain to another.

TABLE 6
Effect of Henry's Constant K_H on Percent VOC Removal

K_H (dimensionless)	Percent VOC removal
0.30	90.28
0.2821 (TCE)	89.71
0.20	85.95
0.10	74.73
0.05	58.23

TABLE 7
Percent VOC Removals from Multiple Curtain Systems

	R_1			
	90	75	50	25
n	R_n			
2	99.00	93.75	75.00	43.75
3	99.90	98.44	87.50	57.81
4	99.99	99.61	93.75	68.36

EFFECTIVE RADIUS OF A SPARGING WELL

Sparging can be carried out by means of a sparging well, which discharges air into the aquifer down near the bottom. One wishes to know the size of the resulting aeration cone, and how this depends on the gas flow rate, in order to design systems using sparging wells. It might be expected that soil gas pressure measurements in the vadose zone in the vicinity of a sparging well might give information on these points, and this in fact turns out to be the case. In this section we explore the soil gas pressure distribution in a cylindrical domain in the vadose zone centered about a single sparging well discharging air well below the water table. See Fig. 2 for a possible set-up, Fig. 3 for the geometry and notation.

The equation governing the pressure of an ideal gas in a porous medium under steady-state conditions is well approximated by

$$0 = \nabla \cdot K \nabla (P^2) \tag{11}$$

This will be solved by approximating it by means of a finite difference representation and then solving the resulting linear equations (in P^2) by a relaxation method. The cylindrically symmetrical geometry and notation are indicated in Fig. 2. The finite difference equation at an interior annular volume element (i,j) is

$$\begin{aligned} 0 = {} & K_r(P^2_{i-1,j} - P^2_{i,j})2\pi(i-1)\Delta z + K_r(P^2_{i+1,j} - P^2_{i,j})2\pi i \Delta z \\ & + K_z(P^2_{i,j-1} - 2P^2_{i,j} + P^2_{i,j+1})(2i-1)\pi \Delta r^2/\Delta z, \\ & i = 2, 3, \ldots, I_r; \qquad j = 2, 3, \ldots, J_z \end{aligned} \tag{12}$$

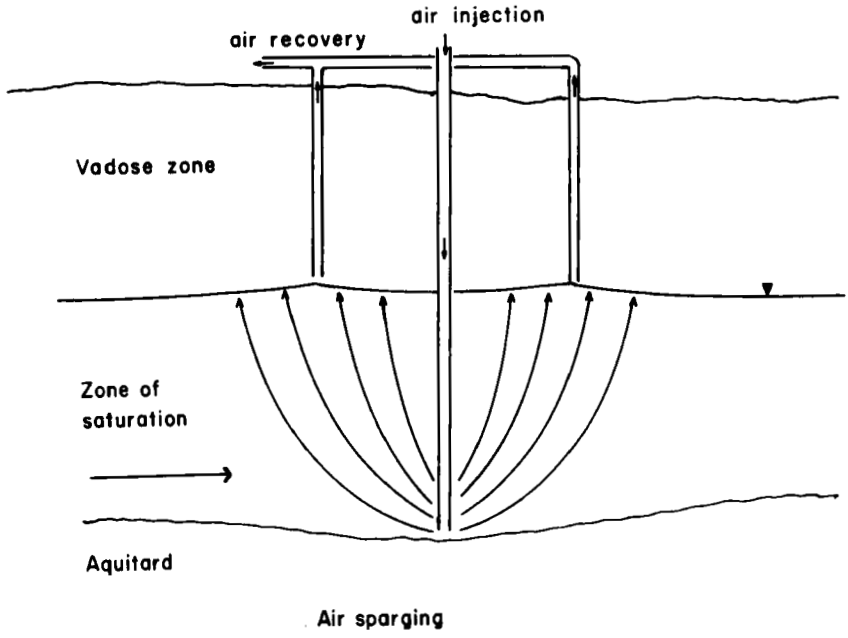

FIG. 2. Sparging with a single air injection well.

Along the axis of the cylindrical domain the equation is

$$0 = K_r(P^2_{i+1,j} - P^2_{i,j})2\pi i\Delta z + K_z(P^2_{i,j-1} - 2P^2_{i,j} + P^2_{i,j+1}) \times (2i - 1)\pi\Delta r^2/\Delta z, \quad i = 1; \quad j = 2, 3, \ldots, J_z - 1 \quad (13)$$

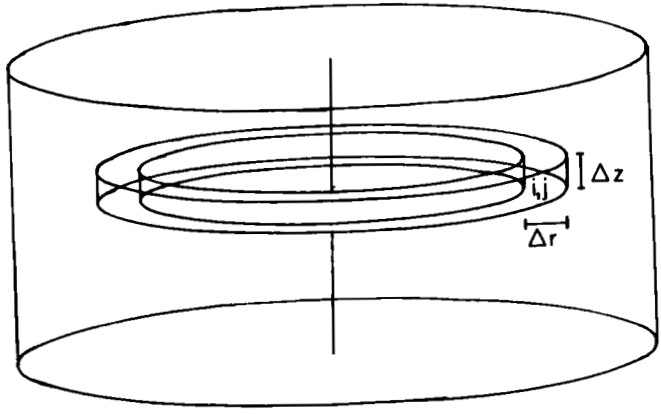

FIG. 3. Mathematical partitioning of the domain of interest in the vadose zone.

If we assume a no-flow boundary condition at the cylindrical periphery of the domain, the equation is

$$0 = K_r(P^2_{i+1,j} - P^2_{i,j})2\pi(i - 1)\Delta z + K_z(P^2_{i,j-1} - 2P^2_{i,j} + P^2_{i,j+1})(2i - 1)\pi\Delta r^2/\Delta z, \quad i = I_r; \quad j = 2, 3, \ldots, J_z - 1 \quad (14)$$

This could be replaced by a boundary condition that the pressure be 1 atm if desired. The development of the difference equations at the boundary is similar to that described above, except that gas flow through the cylindrical periphery is allowed and it is assumed that the gas pressure at this surface is fixed at 1 atm. In doing calculations for single wells, the radius of the cylindrical domain should be taken sufficiently large that the choice of boundary condition is immaterial. We shall explore this point further when we deal with the results. If multiple wells in a hexagonal grid are to be used (each well with six nearest neighbors), the radius of the cylindrical domain should be half the distance between adjacent wells and the no-flow peripheral boundary condition ($\partial P/\partial r = 0$) should be used.

At the bottom of the domain we must include a flux term because of the incoming gas from the sparging well; this gives

$$0 = K_r(P^2_{i-1,j} - P^2_{i,j})2\pi(i - 1)\Delta z + K_r(P^2_{i+1,j} - P^2_{i,j})2\pi i\Delta z + Kyz(P^2_{i,j+1} - P^2_{i,j})(2i - 1)\pi\Delta r^2/\Delta z + Q[(i - 0.5)\Delta r] \times (2i - 1)\pi\Delta r^2, \quad j = 1; \quad i = 2, 3, \ldots, I_r - 1 \quad (15)$$

At the top of the domain the pressure is 1 atm, and the difference equation becomes

$$0 = K_r(P^2_{i-1,j} - P^2_{i,j})2\pi(i - 1)\Delta z + K_r(P^2_{i+1,j} - P^2_{i,j})2\pi i\Delta z + K_z[(P^2_{i,j-1} - P^2_{i,j}) + 2(1 - P^2_{i,j})](2i - 1)\pi\Delta r^2/\Delta z, \quad j = J_z; \quad i = 2, 3, \ldots, I_r \quad (16)$$

In similar fashion one writes four difference equations for the four volume elements (1,1), (1,J_z), (I_r,1), and (I_r,J_z).

Each of these equations is then solved for $P^2_{i,j}$ in terms of the surrounding pressures. One then assumes an expression for the gas flux term at the bottom of the domain, $Q(r)$, assigns a value of unity to all the P^2 , and

iterates the system until convergence has occurred. This is monitored during the course of the calculation by accumulating S, the sum of the squares of the differences between the $P^2_{s,t}$ over all mesh points for successive iterations.

$$S = \sum_{i=1}^{I_r} \sum_{j=1}^{J_z} (P^2_{i,j'} - P^2_{i,j''})^2 \tag{17}$$

where $P^2_{i,j'}$ and $P^2_{i,j''}$ are the kth and the $(k + 1)$th iterated values for $P^2_{i,j}$.

One could speed up convergence by use of an overrelaxation method, but the calculations were sufficiently fast that we did not bother with this elaboration.

The choice of the function $Q(r)$ which specifies the flux coming into the vadose zone domain through its bottom surface is somewhat uncertain. Initially we explored three possibilities, as follows. The first choice was

$$Q(r) = \frac{Q_{\text{tot}}}{4\pi\sigma_r^2} \exp(-r^2/4\sigma_r^2) \tag{18}$$

where Q_{tot} is the total gas flow rate and σ_r gives a measure of the effective radius of the distribution. The second choice was

$$Q(r) = \frac{3Q_{\text{tot}}}{a^3\pi}(a - r), \qquad r < a$$

$$= 0, \qquad r > a \tag{19}$$

The third choice was

$$Q(r) = Q_{\text{tot}}/\pi a^2, \qquad r < a$$

$$= 0, \qquad r > a \tag{20}$$

One can generalize Eq. (19) for $Q(r)$ to explore a broader range of distribution functions by replacing the first power dependence on r by an nth power dependence, as follows.

$$Q(r) = \frac{Q_{\text{tot}}(n + 2)}{\pi a^2 n}[1 - (r/a)], \qquad r < a$$

$$= 0, \qquad r > a \tag{21}$$

The mean radius of $Q(r)$ is given by

$$\bar{r} = \int_0^a Q(r) r^2 dr / Q_{\text{tot}} \tag{22}$$

For Eq. (21) this yields

$$\bar{r} = \frac{2(n + 2)}{3(n + 3)} a \tag{23}$$

which in the limit as n approaches infinity applies to Eq. (20) as well. For Eq. (18), the Gaussian distribution, one obtains

$$\bar{r} = \sqrt{\pi}\sigma_r$$

$$= 1.772\sigma_r \tag{24}$$

We now turn to the results of these calculations. Figure 4 shows plots of soil gas pressure in centimeters of water versus distance from the domain axis at a height 0.5 m above the water table. The Gaussian flux distribution was assumed, and the model parameters are given in Table 8. The gas flow rate from the well was held constant at 0.1 m^3/s for all the runs. It is

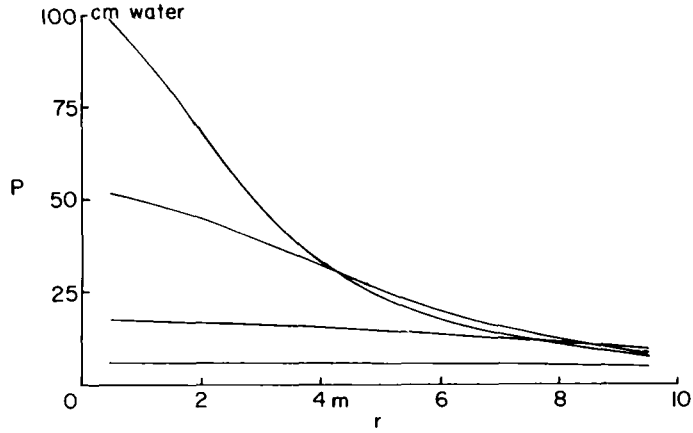

FIG. 4. Effect of σ_r, effective radius parameter, on soil gas pressure distribution 0.5 m above the water table. $Q(r)$ is Gaussian, Eq. (18). From the top down at r = 1 m, σ_r = 1, 2, 5, and 10 m. Other parameters as in Table 8.

TABLE 8
Model Parameters for the Gaussian Gas Flux Calculations

Gas flow rate, Q_{tot}	0.1 m^3/s
Effective radius parameter, σ_r	1, 2, 5, 10 m
Radius of domain of interest	30 m
Horizontal pneumatic permeability, K_r	0.05 $m^3/atm \cdot s$
Vertical pneumatic permeability, K_z	0.05 $m^3/atm \cdot s$

apparent that the soil gas pressure distribution in the vadose zone near the water table depends very strongly on the effective radius parameter of the gas flux distribution at the bottom of the vadose zone.

Figure 5 shows plots of the soil gas pressure (centimeters of water) at a height 0.5 m above the water table versus the distance from the center of the domain for the second, linear, distribution function, given by Eq. (19). The model parameters are as in Table 8, except that the values for the effective radius parameter σ_r were replaced by values of the maximum radius parameter a in Eq. (19); the values of a used were 2, 4, 10, and 20 m.

The results are qualitatively quite similar in appearance to those of Fig. 4, so it seems unlikely that this technique could be used to discriminate between different functional forms of $Q(r)$ with any sensitivity. On the

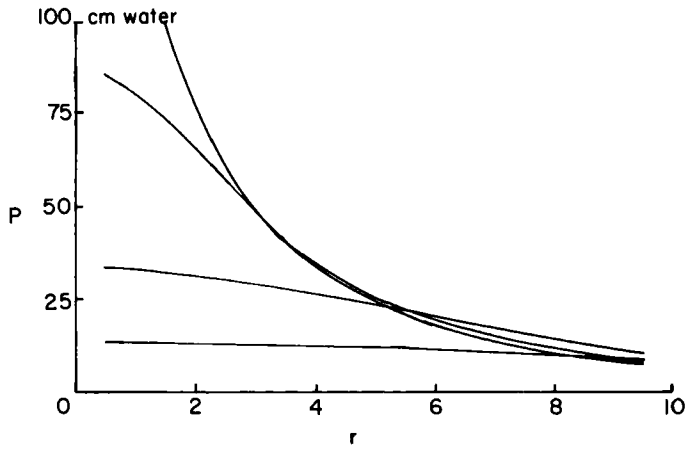

FIG. 5. Effect of a, maximum radius parameter, on soil gas pressure distribution 0.5 m above the water table. $Q(r)$ is a linear function of r, Eq. (19). From the top down at $r = 1$ m, $a = 2$, 4, 10, and 20 m. Other parameters as in Table 8.

other hand, in both Figs. 3 and 4 the radial dependence of the soil gas pressure depends quite strongly on the effective radius of the soil gas flux distribution function $Q(r)$. We therefore conclude that the measurement of soil gas pressures by means of piezometer wells screened near the bottom of the vadose zone should be an effective method for estimating the radius of the gas flow distribution at the water table resulting from a sparging well screened in the zone of saturation.

Figure 6 shows plots of soil gas pressure (centimeters of water) height 0.5 m above the water table versus the distance from the center of the domain for the second, constant, distribution function, given by Eq. (20). The model parameters are as in Table 8, except that the values for the effective radius parameter σ_r were replaced by values of the maximum radius parameter a in Eq. (20); the values of a used were 2, 4, 10, and 20 m. Again we find that the soil gas pressure distribution plots depend very markedly on the radius parameter of $Q(r)$, but that it would be difficult to attempt to distinguish between the different functional forms of $Q(r)$ by means of soil gas pressure measurements.

The effects of the boundary condition used at the cylindrical periphery of the domain are shown in Figs. 7 and 8. The gas flux $Q(r)$ is assumed to be Gaussian, and the parameters used are those given in Table 8. In Fig. 7 the effective radius parameter (σ_r) used is 5 m. In Fig. 8 this parameter is 10 m; this is a least favorable case in that it shows quite marked differences in the soil gas pressures out near the periphery of the domain,

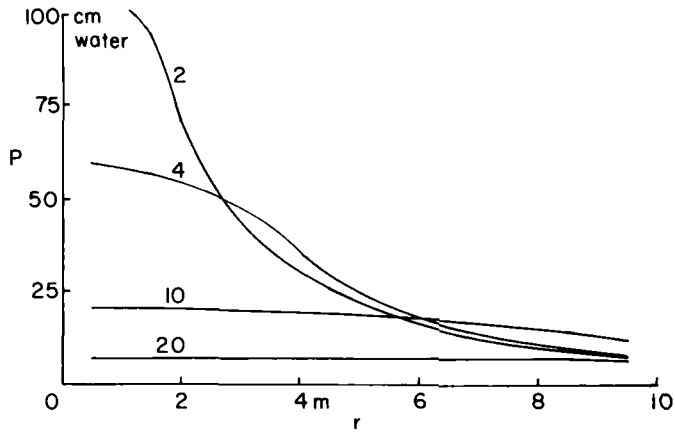

FIG. 6. Effect of a, maximum radius parameter, on soil gas pressure distribution 0.5 m above the water table. $Q(r)$ is a constant for $r < a$, Eq. (20). From the top down at $r = 1$ m, $a =$ 2, 4, 10, and 20 m. Other parameters as in Table 8.

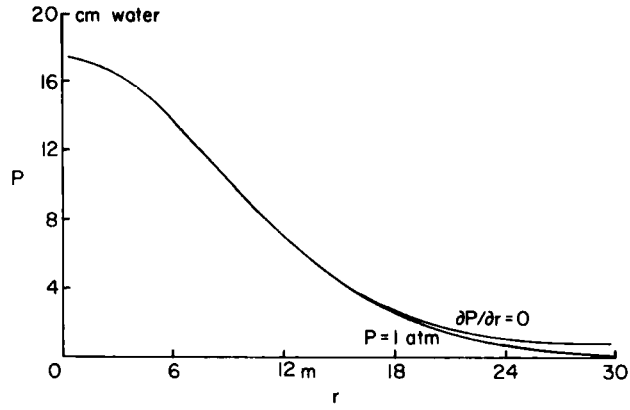

FIG. 7. Effect of boundary condition at domain periphery on soil gas pressure distribution 0.5 m above the water table. $Q(r)$ is Gaussian (Eq. 18), with σ_r = 5 m; other parameters as in Table 8. The boundary condition at r = 30 m for the upper curve is $\partial P/\partial r = 0$; for the lower curve it is P = 1 atm.

say from 20 to 30 m from the sparging well. In Fig. 7, in which σ_r is 5 m, the two different boundary conditions (P = 1 atm and $\partial P/\partial r = 0$) yield quite similar results out almost to the periphery of the domain, at which the soil gas excess pressure from the well has fallen almost to zero anyway. We conclude that the effect of the peripheral boundary condition can be

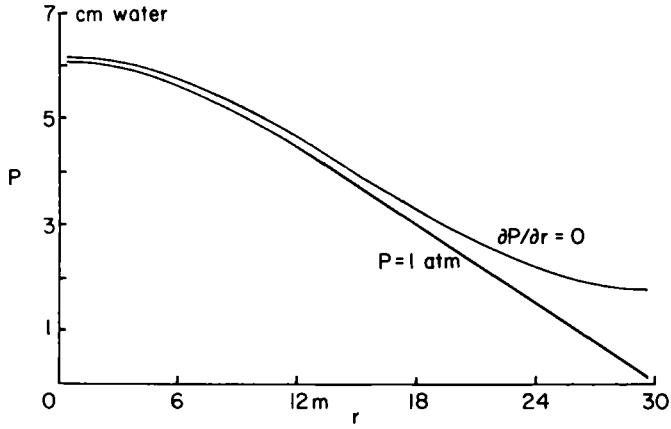

FIG. 8. Effect of boundary condition at domain periphery on soil gas pressure distribution 0.5 m above the water table. $Q(r)$ is Gaussian (Eq. 18), with σ_r = 10 m; other parameters as in Table 8. The boundary condition at r = 30 m for the upper curve is $\partial P/\partial r = 0$; for the lower curve it is P = 1 atm.

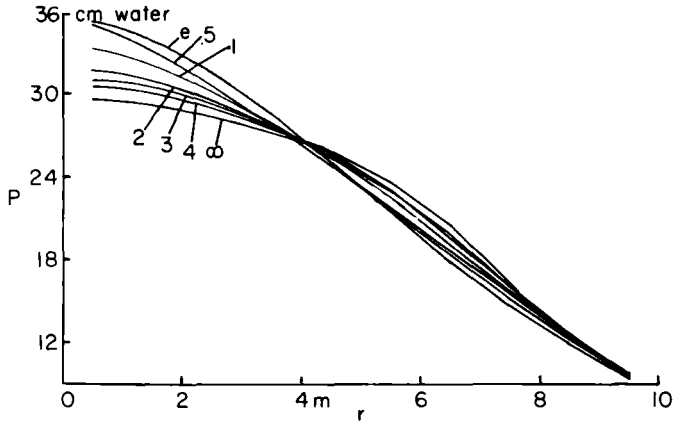

FIG. 9. Effect of the functional form of $Q(r)$ on the soil gas pressure distribution 0.5 m above the water table. $Q(r)$ was calculated by Eq. (18) (Curve e) or by Eq. (21) (all other plots), values of a or σ_r were taken from Table 9, and all other parameters were taken from Table 8.

made unimportant by selecting a domain radius which is substantially larger (say a factor of 5 or 6) than the effective radius parameter σ_r.

The effect of the functional form of $Q(r)$ is explored in Fig. 9. The mean radius of $Q(r)$, given by Eq. (22), was held constant at 5 m, and corresponding values of a or σ_r were calculated for the values of n given in Table 9, and for the Gaussian distribution. Runs were then made using these values of a or σ_r and the other parameters given in Table 8. Figure 9 shows the soil gas pressures 0.5 m above the water table as functions of r for these runs; pressure in excess of 1 atm and measured in centimeters of water is plotted. Note that the pressure scale does not start at 0. For values

TABLE 9
Values of a (and σ_r) Corresponding to $\bar{r}$ = 5 m

n	a (σ_r)
0.5	10.500 m
1	10.000
2	9.375
3	9.000
4	8.750
∞	7.500
(Gaussian)	2.82095 (σ_r)

of r between 10 and 30 m, the curves are virtually superimposed. It is apparent that rather marked changes in the form of the gas distribution function $Q(r)$ result in relatively minor changes in the soil gas pressures in the vadose zone even quite close to the water table. We conclude that, while soil gas pressure measurements appear to be a good probe for determining the effective radius of the spatial distribution of the flow of the injected gas, they are not very sensitive to the details of this distribution.

It is hoped that this method will prove useful to designers of sparging well systems in helping them to estimate the spatial distribution of injected gas in the zone of saturation and the dependence of this distribution on gas flow rate. This, in turn, should be of help in optimizing the design of sparging well systems.

REFERENCES

1. T. G. Naymik, "Mathematical Modeling of Solute Transport in the Subsurface," *CRC Crit. Rev. Environ. Control, 17,* 229 (1987).
2. P. S. Huyakorn, B. H. Lester, and C. R. Faust, "Finite Element Techniques for Modeling Groundwater Flow in Fractured Aquifers," *Water Resour. Res., 19,* 1019 (1983).
3. R. Bibby, "Mass Transport of Solutes in Dual-Porosity Media," *Ibid., 17,* 1075 (1981).
4. A. Rasmuson and I. Neretneiks, "Exact Solution for Diffusion in Particles and Longitudinal Dispersion in Packed Beds," *AIChE J., 26,* 686 (1980).
5. A. Rasmuson and I. Neretneiks, "Migration of Radionuclides in Fissured Rock: The Influence of Micropore Diffusion and Longitudinal Dispersion," *J. Geophys. Res., 86*(B5), 3749 (1981).
6. S. E. Powers, C. O. Louriero, L. M. Abriola, and W. J. Weber Jr., "Theoretical Study of the Significance of Nonequilibrium Dissolution of Nonaqueous Phase Liquids in Subsurface Systems," *Water Resour. Res., 27,* 463 (1991).
7. D. J. Wilson and R. D. Mutch Jr., "Migration of Pollutants in Groundwater. IV. Modeling of the Pumping of Contaminants from Fractured Bedrock," *Environ. Monitor. Assess., 15,* 183 (1990).
8. R. D. Mutch Jr., J. I. Scott, and D. J. Wilson, "Cleanup of Fractured Rock Aquifers: Implications of Matrix Diffusion," *Ibid.,* In press.
9. D. J. Wilson, R. D. Mutch Jr., and J. I. Scott, "Matrix Diffusion Effects in the Cleanup of Heterogeneous Aquifers," *Ibid.,* Submitted.
10. W. J. Lyman and D. C. Noonan, *Assessing UST Corrective Action Technologies: Site Assessment and Selection of Unsaturated Zone Treatment Technologies,* Camp, Dresser & McKee, Inc., EPA/600/2-90/011, Risk Reduction Engineering Laboratory, Cincinnati, Ohio, 1990.
11. T. A. Pedersen and J. T. Curtis, *Soil Vapor Extraction Technology Reference Handbook,* Camp, Dresser & McKee, Inc., EPA/540/2-91/003, Risk Reduction Engineering Laboratory, Cincinnati, Ohio, 1991.
12. B. Herrling and J. Stamm, *Vacuum-Vaporizer-Wells (UVB) for In Situ Remediation of Volatile and Strippable Contaminants in the Unsaturated and Saturated Zones,* Presented at the Symposium on Soil Venting, Houston, Texas, April 29–May 1, 1991, Robert S. Kerr Environmental Research Laboratory and National Center for Ground Water Research, sponsors.

13. R. A. Brown, *Air Sparging—Extending Volatilization to Contaminated Aquifers,* Presented at the Symposium on Soil Venting, Houston, Texas, April 29–May 1, 1991, Robert S. Kerr Environmental Research Laboratory and National Center for Ground Water Research, sponsors.

14. G. B. Howe, M. E. Mullins, and T. N. Rogers, *Evaluation and Prediction of Henry's Law Constants and Aqueous Solubilities for Solvents and Hydrocarbon Fuel Components, Vol. I: Technical Discussion,* USAFESE Report No. ESL-86-66, U.S. Air Force Engineering and Services Center, Tyndall AFB, Florida, 1986, 86 pp.

Received by editor December 12, 1991